(article starts on next page)

Active feedback stabilization of super-efficient microcombs in photonic molecules

ISRAEL REBOLLEDO-SALGADO [1,2], OSKAR B. HELGASON[1], VICENTE DURÁN[3], MARCELLO GIRARDI[1], MARTIN ZELAN[2], AND VICTOR TORRES-COMPANY[1]

[1] *Department of Microtechnology and Nanoscience (MC2), Photonics Laboratory Chalmers University of Technology, SE-412 96, Sweden*
[2] *Measurement Science and Technology, RISE Research Institutes of Sweden, SE-501 15 Borås, Sweden*
[2] *GROC-UJI, Institute of New Imaging Technologies, University Jaume I, 12071 Castellón, Spain*
[*] *israels@chalmers.se*

Dissipative Kerr soliton frequency combs, when generated within coupled cavities, exhibit exceptional performance concerning controlled initiation and power conversion efficiency. Nevertheless, to fully exploit these enhanced capabilities, it is necessary to maintain the frequency comb in a low-noise state over an extended duration. In this study, we demonstrate the control and stabilization of super-efficient microcombs in a photonic molecule. Our findings demonstrate that there is a direct relation between the effective detuning and soliton power, allowing the latter to be used as a set point in a feedback control loop. Employing this method, we achieve the stabilization of a highly efficient microcomb indefinitely, paving the way for its practical deployment in optical communications and dual-comb spectroscopy applications.

1. INTRODUCTION

Dissipative Kerr solitons (DKSs) in microresonators (microcombs) have shown a significant potential for diverse applications, including optical communications, metrology, and sensing, while maintaining a small form factor [1–3]. These applications are enabled through a suite of advantageous features, encompassing a broad optical bandwidth, high repetition rate, and minimal power consumption [4, 5]. DKS microcombs can be generated in microcavities pumped with continuous wave lasers, wherein a delicate equilibrium is achieved through the interplay of the Kerr nonlinear shift with the cavity dispersion, and parametric gain effectively compensating for the cavity losses [6].

Operating in the soliton regime leads to the emergence of phase-locked evenly spaced lines, where the pump laser must be far-red detuned with respect to the pump resonance [6, 7]. This relative detuning governs the soliton formation and the number of solitons circulating the cavity. A single soliton state leads to a thermal self-lock [8] between the pump laser and the resonance maintaining a coherent comb. To maintain a stable soliton state it is critical to control the detuning parameter successfully. Previous works have explored different techniques for this purpose, using Pound-Drever Hall locking [9], or via temperature control using integrated microheaters [10], and monitoring the power of the soliton [11]. The latter approach has been proven to be a successful and simple technique as the power of the soliton has a proportional relationship with the detuning in single cavities [11–14].

Recent works explored new architectures to engineer dispersion profiles using, e.g., coupled cavities [15–17] or through the periodic modulation in the geometry of resonators [18, 19], which has resulted in new microcomb generation dynamics and enhanced performance. In prior work, we presented the utilization of an anomalous dispersion photonic molecule, where two cavities of different sizes are employed to achieve selective mode-splitting [20]. This arrangement, gives rise to two different detuning parameters, effective pump detuning, meaning the frequency distance between the pump laser and the shifted resonance, and comb detuning, defined as the detuning experienced by the other comb lines. By shifting the pump resonance, an enhanced coupling with the pump laser is obtained, increasing the power conversion efficiency of the microcomb.

In this letter, we conduct an experimental investigation into the interplay between the soliton power and the effective detuning in a super-efficient DKS generated in a photonic molecule. We have observed a similar relationship in the comb detuning as previously reported in single cavities. To assess the robustness of this dependence, we have implemented a feedback control, sustaining a solitary soliton state for a 30-hour duration by employing the photodetected soliton power as the set point. Through numerical simulations, we analyze the relation between comb detuning and the soliton power in a coupled cavity and find a scenario akin to that in a single cavity with a Kerr-shifted resonance. Furthermore, the effective pump detuning is characterized using a counter-propagation method where the soliton power is used as a setpoint to change the bandwidth of the frequency comb, resulting in a higher conversion efficiency.

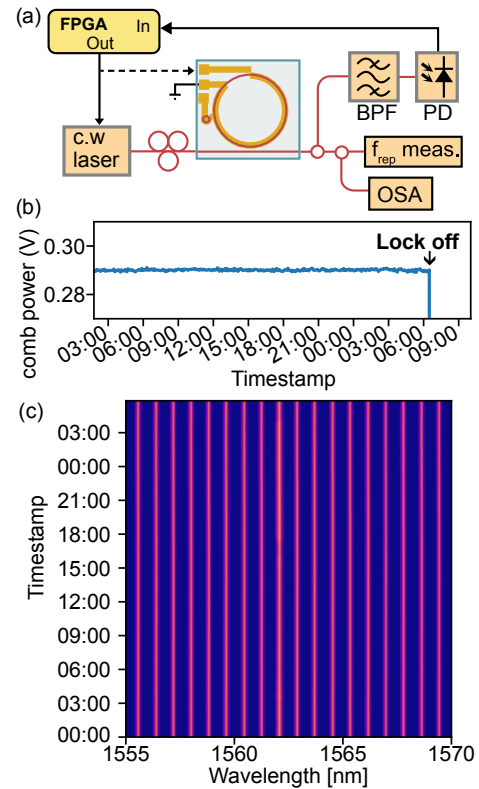In our study we use a photonic molecule composed of two
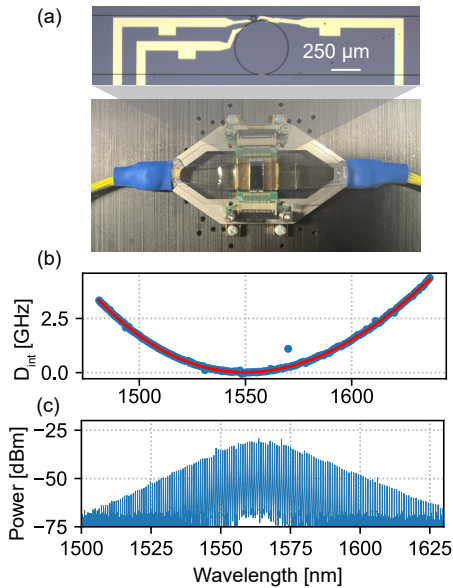
Fig. 1. Super-efficient microcomb module. (a) Photonic molecule packaged into a single module. (b) Measured cold cavity dispersion (D_{int}) of the main cavity. (c) Optical spectrum generated reaching 32 percent of conversion efficiency.

Fig. 2. Long-term stabilization of a super-efficient microcomb.(a) The setup consists of a feedback loop where the soliton power (b) is measured using a photo-detector (PD) and a band-pass filter (BPF). The photo-detected comb power is used as a setpoint to lock the microcomb using a field-programmable-gate-array (FPGA) (c) Soliton state was maintained over 30 hours by acting on the laser.

coupled cavities, main and auxiliary, fabricated in the Si_3N_4 platform using a subtractive method [21–23]. Figure 1 (a) presents the packaged module of the super-efficient photonic molecule. The optical connections of the commercial packaging solution consist of a fiber array followed by a spot-size converter that is edged-coupled to the chip. The total throughput losses are 6.2 dB. The temperature of the chip is stabilized using a thermistor and a thermoelectric cooler integrated into the module. The packaging of the microring resonators allows for keeping a constant throughput power which is an important parameter for the microcomb generation and stabilization [24, 25]. The free spectral range (FSR) of the main cavity and auxiliary cavity corresponds to 99.73 GHz and 970 GHz. As a consequence of the mismatch of the FSR's, a Vernier effect occurs between the longitudinal modes of the cavities, causing a strong avoided mode crossing at a particular mode of the main cavity (see Fig. 1 (b)). This can be observed in the characterized dispersion of the main cavity, where a frequency-calibrated swept-wavelength interferometry method was used [26, 27] (see the measured parameters in Supplemental 1). The frequency comb generated with the photonic molecule is shown in Figure 1 (c).

The experimental setup is depicted in Figure 2 (a), we pumped the microresonator using an external-cavity diode laser (ECDL) at 1563 nm with an on-chip power of 30 mW. The initiation process is similar to the one described in [20], where the laser is tuned from blue towards red. The auxiliary cavity resonance is then brought into proximity to the main cavity, resulting in mode-splitting. This causes a further shift of the pump resonance towards the red. After a single soliton is generated, the optical power is reduced to 15 mW increasing the conversion efficiency. The final spectrum of the comb covers a 20-dB bandwidth of 75 nm with a conversion efficiency (defined as the ratio between the comb power without the pump and the input power) of around 36 percent.

The optical power of the super-efficient microcomb is tapped off for monitoring and locking. Ten percent of the power is

sent to a band-pass filter and a photo-detector. The photo-detected soliton power is then used as a setpoint at the input of a field-programmable gate array (FPGA) board where the signal is processed and a correction signal is generated through a proportional-integral-derivative (PID) control. This system can be implemented with a correction signal applied to act either on the main cavity resonance or in the voltage-controlled piezo of the ECDL (see Fig. 2 (a)). The key aspect is the direct relation between the soliton power and detuning. It is pertinent to mention that our stabilization method is not intended to manipulate the two degrees of freedom of the comb. Rather, this active locking method stabilizes the soliton power and enables long-term operation while the lock is engaged.

The comb power is also monitored using an oscilloscope as shown in Figure 2 (b), where the power remains constant until the control is terminated. Another portion of the optical power is used to monitor the microcomb spectrum using an optical spectrum analyzer (OSA) and its repetition rate using electro-optic down-conversion [28]. The optical spectrum was recorded over the 30 hours the comb was running. As seen in Figure 2 (c) the power of the comb lines remained constant over the whole span.

We performed two experiments to test the robustness of this feedback control. In the first, the feedback was acting on the pump laser frequency, and in the second, it was acting on the
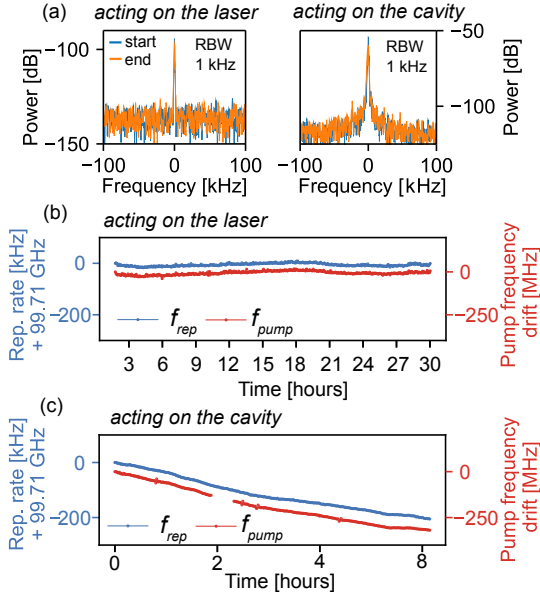
Fig. 3. Characterization of the repetition rate and pump frequencies. (a) Down-converted beat note of the repetition rate of the microcomb when the correction signal is fed back into the piezo control of the laser (left) and to the microheater of the main cavity (right). The measured drift of the frequency of the repetition rate (f_{rep}) is shown in blue and the pump laser (f_{pump}) in red when the microcomb is locked acting on either the laser (b) and acting on the main cavity heater (c).

microheater of the main cavity. Figure 3 (a) shows the down-converted beat notes of the repetition rate frequency. The drift of the repetition rate frequency (f_{rep}) was recorded while the microcomb was locked as shown in 3 (b). Simultaneously, the frequency of the pump laser was measured by heterodyne detection with a self-referenced frequency comb. The beat note (f_{pump}) was recorded using an electrical spectrum analyzer with a resolution bandwidth of 30 kHz. It is readily apparent that the repetition rate frequency follows the frequency of the pump laser, with standard deviations of $\sigma_{f_{rep}} = 5$ kHz and $\sigma_{f_{pump}} = 10$ MHz, respectively. We attribute this effect to the coupling between the pulse rate and the third-order dispersion, which in turn, causes the soliton to experience a different velocity as its central frequency is changed.

We encounter a similar behavior when the microcomb is locked using the cavity heater (Figure 3) (c), where $\sigma_{f_{rep}}$ drifts in a linear manner following the change in frequency of $\sigma_{f_{pump}}$. In this case, we make use of the thermo-optic effect in Si_3N_4 to correct the spectral position of the pumped resonance [10, 29] and maintain the soliton detuning. Since the frequency of the pump laser is not corrected, the f_{pump} beat has a significant drift arising from the thermal cavity expansion of the ECDL triggered by variations in the environmental conditions. An empty region is observed around 150 MHz originating from f_{pump} beat note leaving the measurement window (<250 MHz). Feeding back the error signal to the laser results in a more stable comb than when the error signal is applied to the cavity. We believe this is because cavity drifts are less significant than the laser's.

These two cases show that the coupling between the soliton power and the relative cavity-pump detuning holds in a photonic molecule configuration where a super-efficient soliton is generated. Alternatively to long-term operation, our feed-

back control method can be utilized for tuning the microcomb sustaining a low-noise state [30]. This can be achieved by incorporating a secondary feedback loop to adjust the auxiliary resonance of the photonic molecule (further details provided in the Supplemental document). Implementing the control of the main and auxiliary resonance simultaneously would also enable the correction of large drifts in the pump frequency.
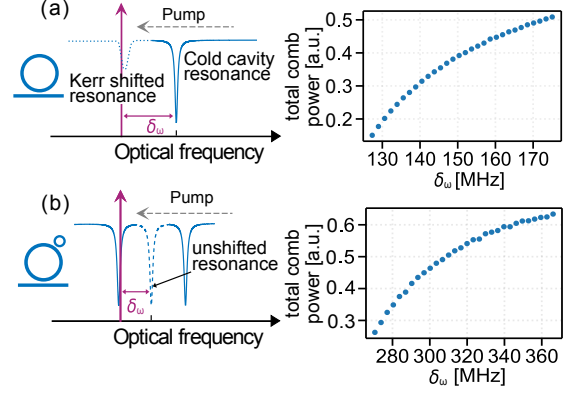
Fig. 4. Soliton power evolution as a function of the detuning. (a) The schematic (left) shows the pump detuning dynamics in a single cavity, where the laser is tuned further from (closer to) the cold cavity (Kerr shifted resonance) causing a soliton power increase (right). (b) In a photonic molecule, a mode-splitting is present causing a shift from a centered resonance. When the laser is tuned further from the unshifted resonance, the soliton detuning increases, and the soliton power grows with a similar trend as in the case of the single cavity.

To better understand our experimental findings, we performed numerical simulations using an Ikeda map [16, 20]. In the first study, a bright DKS was generated in a single cavity, and recorded the out-coupled power as the detuning was increased. This total comb power grows in a sublinear fashion as reported in previous works [11, 13, 14]. The increase in the optical power can be explained as sketched in Figure 4 (a), as the pump laser is tuned further from the cold cavity resonance (increasing δ_ω), it is at the same time getting closer to the Kerr shifted resonance, which determines the soliton duration [14] and causes a more efficient coupling between the laser and the resonance of the cavity modulated by the soliton. In the second case, we simulate the photonic molecule where a shift of the pump resonance is caused by the coupling with an auxiliary cavity. Similarly, as the pump laser is tuned further (see Figure 4 (b)), the soliton detuning δ_ω, i.e. the detuning between the CW laser and the unshifted resonance, the soliton power grows following the same trend as in the single cavity DKS case.

This feedback method can also control the bandwidth of the microcomb since the soliton duration on a resonator also depends on the detuning [14]. We confirmed this relation by measuring directly the laser cavity detuning using a counterpropagating probe laser [31] (Fig. 5 (a)). In Figure 5 (b), a controlled sweep of the detuning is depicted, by changing the operation set-point (soliton power) the bandwidth is selectively controlled as the detuning is changed. As shown in Figure 5 (c), when the frequency separation between the laser and the shifted resonance (δ') is reduced, the pump power is coupled more efficiently causing an increase in the bandwidth (measured above -45 dB in both cases) of the soliton.
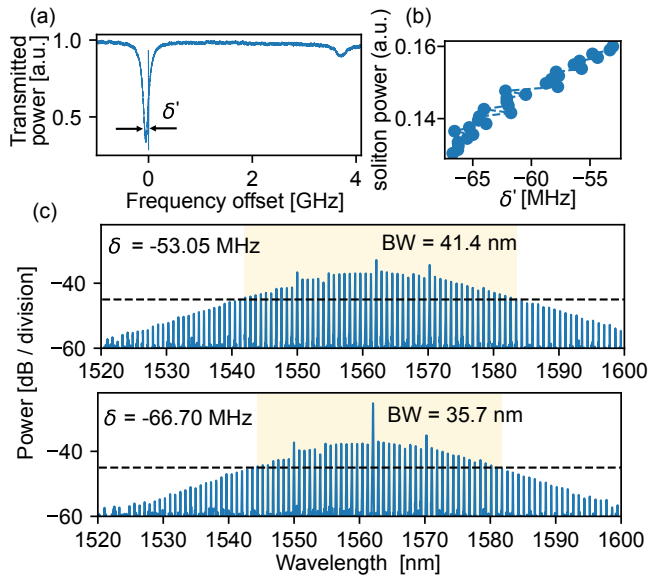
Fig. 5. Pump detuning measurements in a photonic molecule. (a) The transmission power of a blue-detuned resonance was measured using a counter-propagating method. (b) The detuning is measured as the setpoint (soliton power) is tuned to change the pump detuning δ' (c) The soliton bandwidth increases as the pump couples more efficiently into the shifted resonance. The black dashed line is the power threshold used to determine the bandwidth in both cases.

In conclusion, we demonstrate the continuous and stable operation of a super-efficient microcomb over more than one day. We performed an extensive characterization of the locking mechanism using the same principle of operation but with two different approaches, one where the fast fluctuations of the pump frequency are compensated and another where the slow temperature drifts of the cavity are corrected. We find that the coupling between soliton power and the detuning is held in a photonic molecule configuration. These results provide a better understanding of the dynamics of super-efficient microcombs that are not exclusive of photonic molecules but can be attained in other schemes where modal coupling is implemented. We envision that this method can be employed to utilize microcombs in demanding system-level applications.

Disclosures. I.R.S., O.B.H. and V.T.-C. have submitted a patent application based on parts of these results. M.G., O.B.H., and V.T.-C. are co-founders of Iloomina AB.

Data Availability Statement. The data is available in Ref. [32]

REFERENCES

1. A. A. Jørgensen, D. Kong, M. R. Henriksen, F. Klejs, Z. Ye, O. B. Helgason, H. E. Hansen, H. Hu, M. Yankov, S. Forchhammer, P. Andrekson, A. Larsson, M. Karlsson, J. Schröder, Y. Sasaki, K. Aikawa, J. W. Thomsen, T. Morioka, M. Galili, V. Torres-Company, and L. K. Oxenløwe, Nat. Photonics **16**, 798 (2022).

2. D. T. Spencer, T. Drake, T. C. Briles, J. Stone, L. C. Sinclair, C. Fredrick, Q. Li, D. Westly, B. R. Ilic, A. Bluestone, N. Volet, T. Komljenovic, L. Chang, S. H. Lee, D. Y. Oh, M.-G. Suh, K. Y. Yang, M. H. P. Pfeiffer, T. J. Kippenberg, E. Norberg, L. Theogarajan, K. Vahala, N. R. Newbury, K. Srinivasan, J. E. Bowers, S. A. Diddams, and S. B. Papp, Nature **557**, 81 (2018).

3. J. Riemensberger, A. Lukashchuk, M. Karpov, W. Weng, E. Lucas, J. Liu, and T. J. Kippenberg, Nature **581**, 164 (2020).

4. L. Chang, S. Liu, and J. E. Bowers, Nat. Photonics **16**, 95 (2022).

5. Y. Sun, J. Wu, M. Tan, X. Xu, Y. Li, R. Morandotti, A. Mitchell, and D. J. Moss, Adv. Opt. Photonics **15**, 86 (2023).

6. T. J. Kippenberg, A. L. Gaeta, M. Lipson, and M. L. Gorodetsky, Science **361**, eaan8083 (2018).

7. T. Herr, V. Brasch, J. D. Jost, C. Y. Wang, N. M. Kondratiev, M. L. Gorodetsky, and T. J. Kippenberg, Nat. Photonics **8**, 145 (2014).

8. T. Carmon, L. Yang, and K. J. Vahala, Opt. express **12**, 4742 (2004).

9. J. R. Stone, T. C. Briles, T. E. Drake, D. T. Spencer, D. R. Carlson, S. A. Diddams, and S. B. Papp, Phys. Rev. Lett. **121**, 063902 (2018).

10. C. Joshi, J. K. Jang, K. Luke, X. Ji, S. A. Miller, A. Klenner, Y. Okawachi, M. Lipson, and A. L. Gaeta, Opt. Lett. **41**, 2565 (2016).

11. X. Yi, Q.-F. Yang, K. Y. Yang, and K. Vahala, Opt. Lett. **41**, 2037 (2016).

12. C. Bao, L. Zhang, A. Matsko, Y. Yan, Z. Zhao, G. Xie, A. M. Agarwal, L. C. Kimerling, J. Michel, L. Maleki *et al.*, Opt. letters **39**, 6126 (2014).

13. X. Yi, Q.-F. Yang, K. Y. Yang, M.-G. Suh, and K. Vahala, Optica **2**, 1078 (2015).

14. E. Lucas, H. Guo, J. D. Jost, M. Karpov, and T. J. Kippenberg, Phys. Rev. A **95**, 043822 (2017).

15. X. Xue, Y. Xuan, P.-H. Wang, Y. Liu, D. E. Leaird, M. Qi, and A. M. Weiner, Laser & Photonics Rev. **9**, L23 (2015).

16. Ó. B. Helgason, F. R. Arteaga-Sierra, Z. Ye, K. Twayana, P. A. Andrekson, M. Karlsson, J. Schröder, and V. Torres-Company, Nat. Photonics **15**, 305 (2021).

17. I. Rebolledo-Salgado, C. Quevedo-Galán, Ó. B. Helgason, A. Lööf, Z. Ye, F. Lei, J. Schröder, M. Zelan, and V. Torres-Company, Commun. Phys. **6**, 303 (2023).

18. S.-P. Yu, D. C. Cole, H. Jung, G. T. Moille, K. Srinivasan, and S. B. Papp, Nat. Photonics **15**, 461 (2021).

19. E. Lucas, S.-P. Yu, T. C. Briles, D. R. Carlson, and S. B. Papp, Nat. Photonics pp. 1–8 (2023).

20. Ó. B. Helgason, M. Girardi, Z. Ye, F. Lei, J. Schröder, and V. Torres-Company, Nat. Photonics pp. 1–8 (2023).

21. Z. Ye, K. Twayana, P. A. Andrekson *et al.*, Opt. Express **27**, 35719 (2019).

22. A. Gondarenko, J. S. Levy, and M. Lipson, Opt. Express **17**, 11366 (2009).

23. M. Girardi, Ó. B. Helgason, C. H. L. Ortega, I. Rebolledo-Salgado, and V. Torres-Company, arXiv preprint arXiv:2309.02280 (2023).

24. Y. Geng, W. Cui, J. Sun, X. Chen, X. Yin, G. Deng, Q. Zhou, and H. Zhou, Opt. Lett. **45**, 5073 (2020).

25. A. S. Raja, J. Liu, N. Volet, R. N. Wang, J. He, E. Lucas, R. Bouchandand, P. Morton, J. Bowers, and T. J. Kippenberg, Opt. Express **28**, 2714 (2020).

26. P. Del'Haye, O. Arcizet, M. L. Gorodetsky, R. Holzwarth, and T. J. Kippenberg, Nat. Photonics **3**, 529 (2009).

27. K. Twayana, Z. Ye, Ó. B. Helgason, K. Vijayan, M. Karlsson *et al.*, Opt. Express **29**, 24363 (2021).

28. P. Del'Haye, S. B. Papp, and S. A. Diddams, Phys. Rev. Lett. **109**, 263901 (2012).

29. X. Xue, Y. Xuan, C. Wang, P.-H. Wang, Y. Liu, B. Niu, D. E. Leaird, M. Qi, and A. M. Weiner, Opt. express **24**, 687 (2016).

30. I. Rebolledo-Salgado, V. Durán, Ó. B. Helgason, M. Girardi, M. Zelan, and V. Torres-Company, in *2023 CLEO/Europe-EQEC,* (IEEE, 2023), pp. 1–1.

31. P. Del'Haye, A. Coillet, W. Loh, K. Beha, S. B. Papp, and S. A. Diddams, Nat. communications **6**, 5668 (2015).

32. I. Rebolledo-Salgado, "Raw data for: Active feedback stabilization of super-efficient microcombs in photonic molecules," [Data set], Zenodo: Version 1, 16 February 2022 https://doi.org/10.5281/zenodo.6109891.